Dynamical properties and secondary decay effects of projectile fragmentation in ^{107,124}Sn + ^{120}Sn collisions at 600 MeV/nucleon

Jun Su[1], Wolfgang Trautmann[2](*), Long Zhu[1], Wen-Jie Xie[3][4] and Feng-Shou Zhang[5][6][7]

[1] *Sino-French Institute of Nuclear Engineering and Technology, Sun Yat-sen University*
    Zhuhai 519082, China
[2] *GSI Helmholtzzentrum für Schwerionenforschung GmbH - D-64291 Darmstadt, Germany*
[3] *Department of Physics, Yuncheng University - Yuncheng 044000, China*
[4] *Institute of Modern Physics, Chinese Academy of Sciences - Lanzhou 730000, China*
[5] *The Key Laboratory of Beam Technology and Material Modification of Ministry of*
    Education, College of Nuclear Science and Technology, Beijing Normal University,
    Beijing 100875, China
[6] *Beijing Radiation Center - Beijing 100875, China*
[7] *Center of Theoretical Nuclear Physics, National Laboratory of Heavy Ion Accelerator of*
    Lanzhou - Lanzhou 730000, China

Summary. — The formation of the projectile spectator and the fragmentation processes in ^{107,124}Sn + ^{120}Sn collisions at 600 MeV/nucleon are studied with the isospin-dependent quantum molecular dynamics (IQMD) model. The minimum spanning tree algorithm and the ratio of parallel to transverse kinetic quantities are applied to identify the equilibrated projectile spectator during the dynamical evolution. The influence of secondary decay on fragmentation observables is investigated by performing calculations with and without the statistical code GEMINI. The validity of the theoretical approach is examined by comparing the calculated product yields and correlations with the experimental results of the ALADIN Collaboration for the studied reactions.

1. – Introduction

The quantum-molecular-dynamics (QMD) transport model has been very successful in describing heavy-ion reactions at intermediate and higher energies. For example, the multifragmentation following collisions of ^{197}Au + ^{197}Au nuclei at 60 to 150 MeV/nucleon,

(*) E-mail: w.trautmann@gsi.de

measured by the INDRA-ALADIN Collaboration, has been quantitatively reproduced [1]. The FOPI data on particle production and flow in heavy-ion reactions at energies up to 1.5 GeV/nucleon were successfully interpreted with the IQMD model [2,3] and information on the nuclear equation of state (EOS) was deduced from comparisons with IQMD [3,4] and UrQMD predictions [5]. The density dependence of the nuclear symmetry energy up to nearly twice the saturation density was investigated by analyzing elliptic flows of neutrons and light charged particles in ^{197}Au + ^{197}Au collisions at 400 MeV/nucleon with the UrQMD and Tübingen QMD models [6,7].

A puzzle that existed for many years is posed by the apparent inability of the QMD model to describe the socalled rise and fall of fragment formation in projectile fragmentation at relativistic energies in the 1 GeV/nucleon regime with a standard minimum-spanning-tree (MST) algorithm. Begemann-Blaich *et al.* concluded in 1993 that "it is not possible to reproduce the fragment distributions" in the fragmentation of ^{197}Au nuclei at 600 MeV/nucleon measured by the ALADIN Collaboration [8]. A method of circumventing the problem presented by several authors is based on the early fragment recognition suggested by Dorso and Randrup [9]. Appropriate algorithms are used to identify fragmented structures that emerge in the colliding system at times of typically 60 fm/c after the first impact. With the SACA (Simulated Annealing Cluster Algorithm, ref. [10]) or, more recently, the FRIGA (Fragment Recognition In General Application, ref. [11]) algorithms the production of intermediate mass fragments over the full range of impact parameters could be satisfactorily reproduced [11-13].

In a very recent paper [14], a study of projectile fragmentation in the reactions ^{107,124}Sn + ^{120}Sn at 600 MeV/nucleon within the framework of the IQMD model [15,16] plus GEMINI code [17] was presented. The IQMD-BNU (Beijing Normal University) code was used [18], a version introduced and compared to other QMD versions within the transport-code-comparison project [19]. The GEMINI model was applied to simulate the decays of the prefragments and the MST method was used for identifying the final products. Not only the properties of the projectile spectator but also the fragmentation processes were identified, and it was shown that the experimental results of the ALADIN Collaboration for the studied reactions [20] are very satisfactorily reproduced. In this contribution, a brief summary of the study is presented together with first results of an investigation of how to resolve the MST puzzle.

2. – The reaction model

The theoretical framework developed for the present study is described in detail in ref. [14]. The parameters chosen for the IQMD description provide a compressibility of 200 MeV at saturation density (without momentum-dependent interactions) for symmetric nuclear matter. The potential part of the symmetry energy has a value of 19.0 MeV at saturation density and its density dependence is modeled as a power law with exponent $\gamma_i = 0.75$. Together with the kinetic energy, it provides the symmetry energy 31.6 MeV and slope 67.9 MeV at saturation density. The consequences of varying these parameters are presently under study.

The isospin and in-medium dependent parametrization of the elastic nucleon-nucleon (NN) cross sections is taken from refs. [21,22]. To account for the fermionic nature of nucleons, the method of the phase-space density constraint (PSDC) of the constrained molecular dynamics (CoMD, ref. [23]) model is applied. The phase-space occupation probability $\overline{f}_i$ is calculated by performing the integration on a hypercube of volume h^3 in the phase space centered around the i-th nucleon at each time step. If the phase-

space occupation $\overline{f}_i$ has a value greater than unity, the momentum of the i-th nucleon is changed randomly by many-body elastic scattering. This is done for all nucleons at each time step. In the case of collisions, the Pauli blocking of the final states is taken into account. The simulations of the IQMD code are stopped when the excitation energies of the two heaviest prefragments are less than a specified value E_{stop}, chosen to have values between 2 and 4 MeV/nucleon. At that time, the GEMINI code is switched on to follow the deexcitation of the formed prefragments.

3. – Results and discussion

In the IQMD model, the positions and momenta of the nucleons as a function of time can be obtained. At any time during the reaction process, fragments can be recognized by a minimum spanning tree (MST) algorithm, in which nucleons with relative distance of coordinate and momentum of $|r_i - r_j| \leq R_0$ and $|p_i - p_j| \leq P_0$ are considered as belonging to the same fragment [15]. The adopted values $R_0 = 3.5$ fm and $P_0 = 250$ MeV/c are phenomenological parameters. The MST algorithm is performed during the collision and the mass and excitation energies of the identified fragments are determined. The ratio of parallel to transverse quantities is further used to distinguish the equilibrated projectile spectator:

$$(1) \qquad R_E = \frac{2 \sum_i (p_{zi} - p_{zf})^2}{\sum_i \left[(p_{xi} - p_{xf})^2 + (p_{yi} - p_{yf})^2 \right]},$$

where p_{xi}, p_{yi}, and p_{zi} are the momentum components of the i-th nucleon along the x, y, and z-axes; p_{xf}, p_{yf}, and p_{zf} are the average momentum per nucleon of the fragment along the same axes. The summation includes all nucleons of the considered fragment. The z-axis is the direction of incidence of the projectile. For an equilibrated system, the value of R_E approaches unity.

The temporal evolution of R_E is calculated for each event in the IQMD model. As an example, the ratio R_E obtained for the heaviest fragment is shown in fig. 1 (upper panel) for three events of ^{124}Sn + ^{120}Sn collisions at 600 MeV/nucleon with impact parameter $b = 5$ fm. Before the collision takes place, the identified heaviest fragment is the projectile with R_E close to unity. In the dynamical and nonequilibrium stage (from 10 to about 40 fm/c), the heaviest "fragment" is the colliding system with a parallel energy close to the incident energy. After the projectile spectator is separated from the participant region, it equilibrates and its value of R_E decreases towards unity. In the actual calculations, projectile spectators with $0.9 < R_E < 1.2$ were regarded as equilibrated.

The distributions of equilibration times for three impact parameters are shown in fig. 1 (bottom panel). For central ($b = 0$ fm), mid-peripheral ($b = 5$ fm), and peripheral ($b = 10$ fm) collisions, they are located in the interval $20 < t < 150$ fm/c. For peripheral collisions, inelastic scattering results in a peak of the distribution near $t = 25$ fm/c.

After equilibration is observed, subsequent fragmentation processes may be described statistically. In the present case, only the final deexcitation of spectator fragments is described with the GEMINI code. To show the role of the GEMINI code, we compare results before and after GEMINI has been used. The correlation of the mean multiplicity of intermediate mass fragments ($3 \leq Z \leq 20$) with the total bound charge Z_{bound} in the event is shown for ^{124}Sn + ^{120}Sn collisions at 600 MeV/nucleon in fig. 2. The variable Z_{bound} represents the sum of the atomic numbers of products with $Z \geq 2$ and, being close to the atomic number of the disintegrating projectile spectator, is monotonically correlated with the impact parameter [24]. The experimental data for the same reaction,
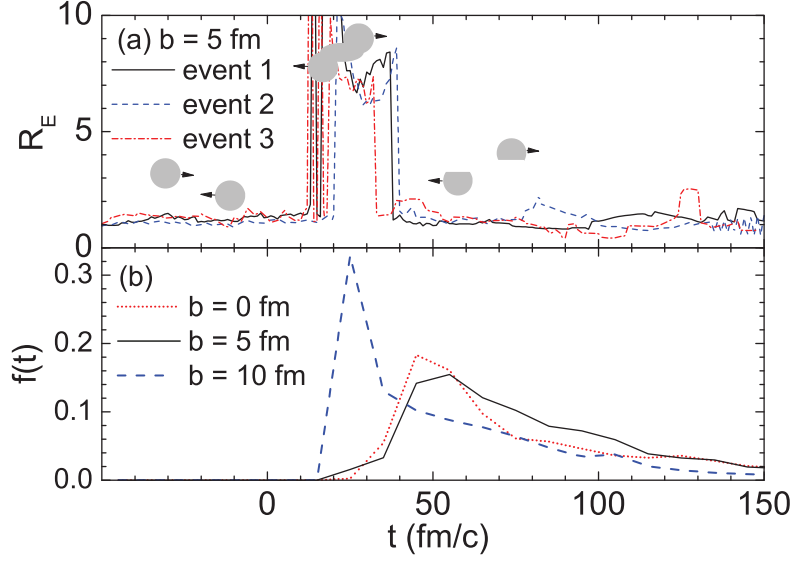
Fig. 1. – (a) Temporal evolution of R_E of the heaviest fragment (or system) in three events of ^{124}Sn + ^{120}Sn collisions at $600\,\text{MeV/nucleon}$ with impact parameter $b = 5\,\text{fm}$. (b) Distribution of equilibration times for the projectile spectator in the same reaction with impact parameters $b = 0, 5$, and $10\,\text{fm}$.

performed with a natural Sn target (atomic weight 118.7), are taken from ref. [20]. The acceptance of the ALADIN forward spectrometer for projectile fragments is large. By studying angular distributions measured for the present reactions, it was found to increase with Z from about 90% for projectile fragments with $Z = 3$ to values exceeding 95% for $Z \geq 6$ [24].
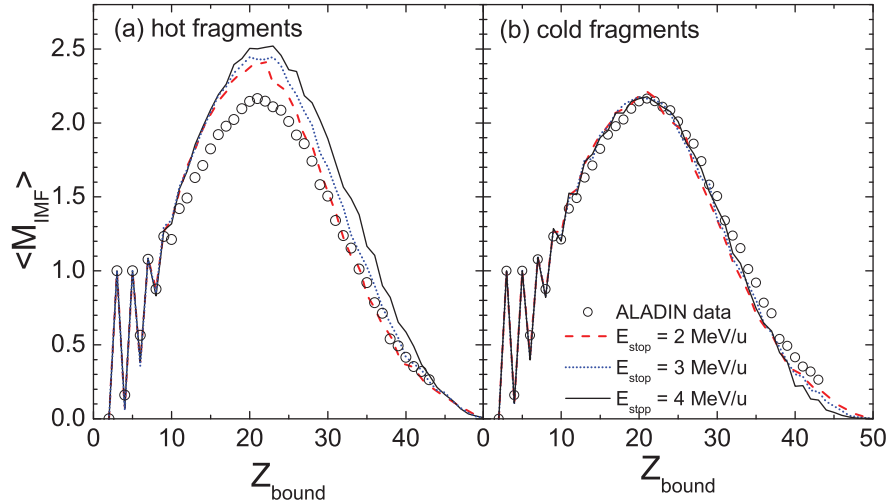

Fig. 2. – Mean multiplicity $\langle M_{\text{IMF}} \rangle$ of intermediate-mass fragments ($3 \leq Z \leq 20$) as a function of Z_{bound} for reactions of ^{124}Sn + ^{120}Sn at $600\,\text{MeV/nucleon}$ as obtained with (a) IQMD and (b) IQMD+GEMINI. The calculations were performed for three values of E_{stop} as indicated. The experimental data (open circles) are taken from ref. [20].

The multiplicities exhibit the rise and fall of the fragment production. The lower multiplicities for smaller values of Z_{bound} indicate the presence of vaporization events in central collisions, while those in the $Z_{\mathrm{bound}} > 40$ region indicate inelastic events in peripheral collision. The data strongly stagger for $Z_{\mathrm{bound}} < 10$. This phenomenon is caused by the definition of Z_{bound} which includes the charge of observed α particles whose number is not included in M_{IMF}. In particular, we observe that the MST method as applied in the present study is capable of reproducing the fragment production over the full range of Z_{bound}, in contrast to refs. [8, 12, 13]. The reason for the difference is not fully clear at present but is, most likely, related to the PSDC method applied to account for the Pauli principle (see below). The nearly negligible isotopic effect seen in a comparison of the M_{IMF} *vs.* Z_{bound} distributions for the two reactions with ^{107}Sn and ^{124}Sn projectiles [20, 25] is also well reproduced by the calculations [14].

The cross sections $\mathrm{d}\sigma/\mathrm{d}Z$ obtained for the fragments produced in the ^{124}Sn + ^{120}Sn reaction are shown in fig. 3 after sorting into five intervals of Z_{bound}. The calculations are again shown with and without the use of GEMINI. Overall, the model calculations reproduce the data rather satisfactorily with a quality comparable to that of the statistical description presented by Ogul *et al.* [20] or Mallik *et al.* [26]. Only the experimental cross sections of the most peripheral collisions ($Z_{\mathrm{bound}} \geq 40$) are somewhat underrepresented. The effect of choosing different values of E_{stop} is very small, as illustrated in figs. 2 and 3. It may be concluded that the deexcitation of moderately excited fragments with excitation energies between 2 and 4 MeV/nucleon is adequately reproduced with both, the IQMD and GEMINI codes. The main effect of GEMINI, as observed in the figures, is the small reduction of the fragment multiplicity, caused by the breakup of some of the lighter fragments in the final deexcitation stage.
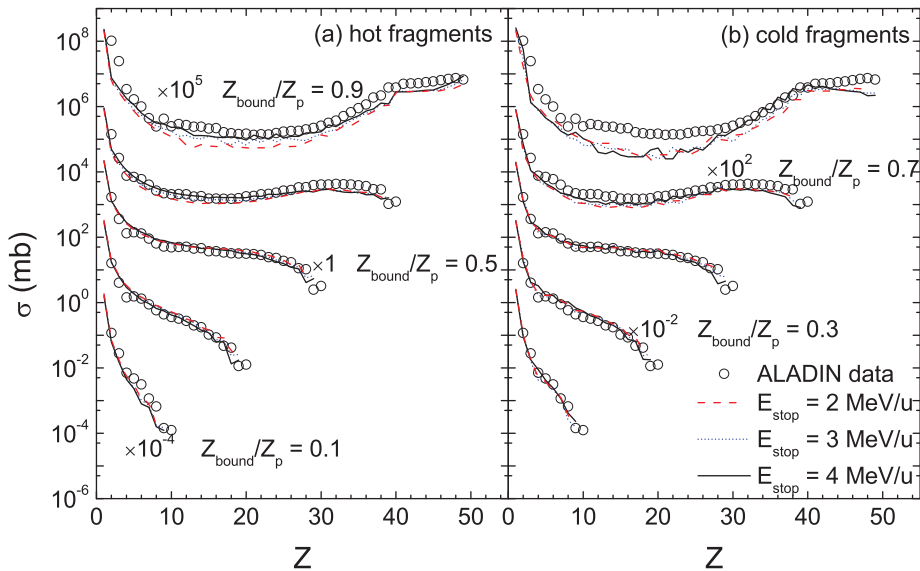

Fig. 3. – Calculated cross sections $\mathrm{d}\sigma/\mathrm{d}Z$ for the fragments produced in the reaction ^{124}Sn + ^{120}Sn at 600 MeV/nucleon in comparison with the experimental data. The events are sorted into five intervals of Z_{bound}/Z_p with centers as indicated and width 0.2 ($Z_p = 50$ is the atomic number of the projectile). The calculations with IQMD and with IQMD+GEMINI are shown in the left and right panels, respectively. The experimental data are taken from ref. [20].
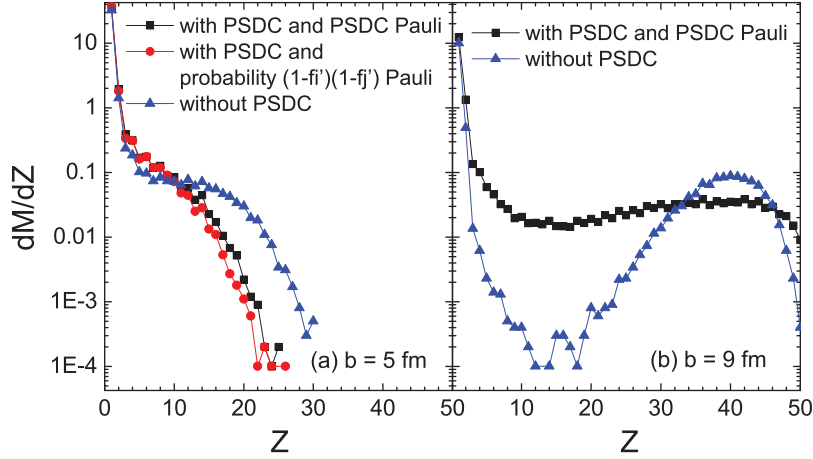
Fig. 4. – Differential fragment multiplicity dM/dZ, calculated with the indicated methods to account for the Pauli principle, in the reaction ^{124}Sn + ^{120}Sn at 600 MeV/nucleon for impact parameters $b = 5$ fm (a) and $b = 9$ fm (b).

4. – PSDC and fragmentation

In the case of collisions, the Pauli blocking of the final states has to be taken into account. Different algorithms are being used for this purpose. In the original IQMD [16], collisions are allowed with the probability $(1-f'_i)(1-f'_j)$; here f'_i and f'_j are the phase space densities at the final states before the scattered particle is placed there. The Pauli blocking method related to the PSDC is used in the present work. These two methods have been compared in our previous work [27]. The Pauli blocking method related to the PSDC is consistent with our using the PSDC method throughout the reaction to account for the fermionic nature of nucleons. It is required that no state with $\overline{f}_i > 1$ is created in a binary NN collision, otherwise it will be changed by the PSDC method. Thus, for each binary NN collision the phase space occupation probabilities $\overline{f}_i$ and $\overline{f}_j$ at the final states are measured. Only if $\overline{f}_i$ and $\overline{f}_j$ at the final states are both less than 1, the scattering is accepted.

The effects on fragment production following from choosing either one or the other method are illustrated in fig. 4 with calculations performed for fixed impact parameters $b = 5$ and 9 fm. In particular at the larger impact parameter, the obtained multiplicities of intermediate-mass fragments depend strongly on this choice. They are systematically lower in calculations without PSDC than with PSDC, while the yield of heavy residue-type fragments is larger if the PSDC is not applied (blue triangles). Whether the probability method or the PSDC is used for collisions seems to have a minor effect (red dots and black squares, respectively, in the left panel). The underlying reason for the strong consequences following from applying the PSDC at each time step is still under investigation.

$$* \ * \ *$$

REFERENCES

[1] ZBIRI K. *et al.*, *Phys. Rev. C*, **75** (2007) 034612.
[2] REISDORF W. *et al.*, *Nucl. Phys. A*, **848** (2010) 366.
[3] REISDORF W. *et al.*, *Nucl. Phys. A*, **876** (2012) 1.
[4] LE FÈVRE A., LEIFELS Y., REISDORF W., AICHELIN J. and HARTNACK CH., in *Proceedings of the IWM-EC2016 International Workshop on Multi facets of EoS and Clustering, GANIL (Caen, France), 9–12 May 2016*, edited by CHBIHI A., LOPEZ O., PAGANO A., PIRRONE S., RUSSOTTO P. and VERDE G., *Nuovo Cimento C*, **39** (2016) 399.
[5] YONGJIA WANG, CHENCHEN GUO, QINGFENG LI, LE FÈVRE A., LEIFELS Y. and TRAUTMANN W., *Phys. Lett. B*, **778** (2018) 207.
[6] RUSSOTTO P. *et al.*, *Phys. Rev. C*, **94** (2016) 034608.
[7] COZMA M. D., *Eur. Phys. J. A*, **54** (2018) 40.
[8] BEGEMANN-BLAICH M. *et al.*, *Phys. Rev. C*, **48** (1993) 610.
[9] DORSO C. and RANDRUP J., *Phys. Lett. B*, **301** (1993) 328.
[10] PURI RAJEEV K., HARTNACK CH. and AICHELIN J., *Phys. Rev. C*, **54** (1996) R28.
[11] LE FÈVRE A., LEIFELS Y., AICHELIN J., HARTNACK CH. and KIREYEV V., *Nucl. Phys. A*, **945** (2016) 112.
[12] GOSSIAUX P. B., PURI R., HARTNACK CH. and AICHELIN J., *Nucl. Phys. A*, **619** (1997) 379.
[13] VERMANI YOGESH K. and PURI RAJEEV K., *EPL*, **85** (2009) 62001.
[14] JUN SU, TRAUTMANN W., LONG ZHU, WEN-JIE XIE and FENG-SHOU ZHANG, *Phys. Rev. C*, **98** (2018) 014610.
[15] AICHELIN J., *Phys. Rep.*, **202** (1991) 233.
[16] HARTNACK CH., PURI RAJEEV K., AICHELIN J., KONOPKA J., BASS S. A., STÖCKER H. and GREINER W., *Eur. Phys. J. A*, **1** (1998) 151.
[17] CHARITY R. J. *et al.*, *Nucl. Phys. A*, **483** (1988) 371.
[18] JUN SU, CHEREVKO K., WEN-JIE XIE and FENG-SHOU ZHANG, *Phys. Rev. C*, **89** (2014) 014619.
[19] JUN XU. *et al.*, *Phys. Rev. C*, **93** (2016) 044609.
[20] OGUL R. *et al.*, *Phys. Rev. C*, **83** (2011) 024608; **85** (2012) 019903(E).
[21] CUGNON J., L'HÔTE D. and VANDERMEULEN J., *Nucl. Instrum. Methods Phys. Res. B*, **111** (1996) 215.
[22] COUPLAND D. D. S., LYNCH W. G., TSANG M. B., DANIELEWICZ P. and YINGXUN ZHANG, *Phys. Rev. C*, **84** (2011) 054603.
[23] PAPA M., MARUYAMA T. and BONASERA A., *Phys. Rev. C*, **64** (2001) 024612.
[24] SCHÜTTAUF A. *et al.*, *Nucl. Phys. A*, **607** (1996) 457.
[25] SFIENTI C. *et al.*, *Phys. Rev. Lett.*, **102** (2009) 152701.
[26] MALLIK S., CHAUDHURI G. and DAS GUPTA S., *Phys. Rev. C*, **84** (2011) 054612.
[27] JUN SU and FENG-SHOU ZHANG, *Phys. Rev. C*, **87** (2013) 017602.